

1 Biogeochemical characteristics of a Long-lived 2 anticyclonic eddy in the eastern South Pacific 3 Ocean

4 *Marcela Cornejo D'Ottone*, Escuela de Ciencias del Mar, Pontificia Universidad Católica de
5 Valparaíso, P.O. Box 1020, Valparaíso Chile and Millennium Institute of Oceanography,
6 Chile (IMO).

7 *Luis Bravo*, Centro de Estudios Avanzados en Zonas Áridas (CEAZA), Facultad de Ciencias del
8 Mar, Universidad Católica del Norte & Millennium Nucleus for Ecology and Sustainable
9 Management of Oceanic Islands (ESMOI), Coquimbo, Chile.

10 *Marcel Ramos*, Departamento de Biología Marina, Facultad de Ciencias del Mar,
11 Universidad Católica del Norte & Millennium Nucleus for Ecology and Sustainable
12 Management of Oceanic Islands (ESMOI) & Centro de Estudios Avanzados en Zonas Áridas
13 (CEAZA), Coquimbo, Chile.

14 *Oscar Pizarro*, Department of Geophysics, University of Concepcion, Chile and Millennium
15 Institute of Oceanography, Chile (IMO).

16 *Johannes Karstensen*, GEOMAR Helmholtz Centre for Ocean Research Kiel, Kiel, Germany

17 *Mauricio Gallegos*, Departamento de Ecología, Pontificia Universidad Católica de Chile,
18 Santiago, Chile.

19 *Marco Correa-Ramirez*, Escuela de Ciencias del Mar, Pontificia Universidad Católica de
20 Valparaíso, P.O. Box 1020, Valparaíso, Chile and Instituto Milenio de Oceanografía (IMO).

21 *Nelson Silva*, Escuela de Ciencias del Mar, Pontificia Universidad Católica de Valparaíso, P.O.
22 Box 1020, Valparaíso Chile.

23 *Laura Farias* Departamento de Oceanografía, Centro ciencia de Clima y la Resielcia (CR2)
24 and Instituto Milenio de Oceanografia (IMO).

25 *Lee Karp-Boss*, School of Marine Science, University of Maine, Orono, ME 04469, USA

26 **ABSTRACT**

27 Mesoscale eddies are important, frequent, and persistent features of the circulation in the
28 eastern South Pacific (ESP) Ocean, transporting physical, chemical and biological properties
29 from the productive shelves to the open ocean. Some of these eddies exhibit subsurface
30 hypoxic or suboxic conditions and may serve as important hotspots for nitrogen loss, but
31 little is known about oxygen consumption rates and nitrogen transformation processes
32 associated with these eddies. In the austral fall of 2011, during the Tara Oceans expedition,
33 an intrathermocline, anticyclonic, mesoscale eddy with a suboxic ($<2 \mu\text{mol kg}^{-1}$ of O_2),
34 subsurface layer (200-400 m) was detected ~ 900 km off the Chilean shore (30°S , 81°W). The
35 core of the eddy's suboxic layer had a temperature-salinity signature characteristic of
36 Equatorial Subsurface Water (ESSW) that at this latitude is normally restricted to an area
37 near the coast. Measurements of nitrogen species within the eddy revealed
38 undersaturation (below 44%) of nitrous oxide (N_2O) and nitrite accumulation ($> 0.5 \mu\text{M}$),
39 suggesting that active denitrification occurred in this water mass. Using satellite altimetry,
40 we were able to track the eddy back to its region of formation on the coast of central Chile
41 (36.1°S , 74.6°W). Field studies conducted in Chilean shelf waters close to the time of eddy
42 formation provided estimates of initial O_2 and N_2O concentrations of the ESSW source water
43 in the eddy. By the time of its offshore sighting, concentrations of both O_2 and N_2O in the
44 subsurface oxygen minimum zone (OMZ) of the eddy were lower than concentrations in
45 surrounding water and 'source water' on the shelf, indicating that these chemical species
46 were consumed as the eddy moved offshore. Estimates of apparent oxygen utilization rates
47 at the OMZ of the eddy ranged from 0.29 to 44 $\text{nmol L}^{-1} \text{d}^{-1}$ and the rate of N_2O consumption

48 was 3.92 nmol L⁻¹ d⁻¹. These results show that mesoscale eddies affect open-ocean
49 biogeochemistry in the ESP not only by transporting physical and chemical properties from
50 the coast to the ocean interior but also during advection, local biological consumption of
51 oxygen within an eddy further generates conditions favorable to denitrification and loss of
52 fixed nitrogen from the system.

53 INTRODUCTION

54 Mesoscale eddies play a major role in vertical and horizontal transport of heat, salts and
55 other physical, chemical and biological constituents (Chelton et al., 2007; Chaigneau et al.,
56 2008, 2009). In the eastern South Pacific (ESP) Ocean, mesoscale eddies frequently form in
57 the coastal transition zone off central Chile due to the instability of the alongshore currents
58 (Hormazábal et al., 2013; Morales et al., 2010, 2012). These eddies transport water for long
59 distances and over several months across biogeographic boundaries, from the productive
60 Humboldt (Peru-Chile) Current to adjacent oligotrophic waters of the subtropical gyre
61 (Pizarro et al., 2006). While cyclonic eddies transport surface waters and are seen as
62 negative anomalies by altimetry data, anticyclonic eddies, including the Intrathermocline
63 eddies (ITE) are deeper and transport low oxygen and salty subsurface waters from the
64 Equatorial Subsurface Waters (ESSW) (Chaigneau et al., 2011).

65 Although eddies have been considered a net loss of nutrients from the coastal zone (Gruber,
66 2011), they constitute a nutrient source in the open ocean that stimulates production in
67 oligotrophic regions (McGillicuddy et al., 1998). In addition, eddies introduce spatial
68 heterogeneity in productivity, community structure and particle flux, as has been observed
69 in the Sargasso Sea (McGillicuddy et al., 1998; Sweeney et al., 2003). Impacts of eddies on
70 biogeochemical processes are of particular interest for coastal transition zones of eastern
71 boundary currents, where oxygen minimum zones (OMZs) and eddies interact (Altabet et
72 al., 2012; Stramma et al., 2013). Open-ocean eddies associated with subsurface hypoxic or
73 suboxic conditions have been observed in both the eastern tropical Atlantic and eastern
74 tropical Pacific (e.g., Lukas and Santiago-Mandujano 2001; Stramma et al., 2014; Karstensen

75 et al., 2015). High surface productivity, downward particle flux and oxygen respiration,
76 combined with sluggish exchange between the eddy interior and surrounding waters, have
77 been proposed as mechanisms leading to the formation of "dead zones" observed within
78 anticyclonic-mode water eddies (Karstensen et al., 2015). Oxygen consumption rates within
79 an eddy can be 3 to 5 times higher than in the surrounding oligotrophic water (Karstensen
80 et al., 2015). Eddies containing hypoxic or suboxic water can become hotspots for nitrogen
81 cycling, including biogenic production of N_2 and loss of fixed nitrogen from the system
82 (Altabet et al., 2012; Stramma et al., 2013). Recently, Stramma et al. (2013) suggested that
83 in the eastern tropical Pacific Ocean, coastal mode water eddies are zones of active loss of
84 fixed nitrogen while nitrogen loss associated with older, open ocean mode water eddies is
85 considerably lower .

86 In eastern boundary subtropical upwelling systems with a pronounced subsurface OMZ,
87 such as in the ESP, eddies may play an important role in transporting OMZ waters and their
88 microbial communities to the open ocean. The OMZ in the upwelling region of the ESP is
89 associated with Equatorial Subsurface Water (ESSW) that has been transported poleward,
90 from the Pacific Ocean equatorial belt, along the coast with the Peru-Chile undercurrent.
91 The ESSW is characterized by high salinity and nutrient concentrations, low oxygen
92 concentrations and an active, bacterially mediated nitrogen cycling, including production
93 and consumption of the greenhouse gas nitrous oxide (N_2O). Intense nitrification,
94 denitrification and nitrous oxide (N_2O) production associated with ESSW is generally
95 confined to a narrow coastal band and contributes to net nitrogen loss in this region (Lam
96 and Kuypers, 2011).

97 Intriguing questions about the role of coastally generated eddies abound: What
98 biogeochemical transformations occur as this volume of water is advected offshore? Do
99 concentrations of dissolved oxygen decrease, increase or remain the same? If changes in
100 dissolved oxygen concentrations occur during transport, what are other biogeochemical
101 consequences in both surface and subsurface layers? Here, we present results from a study
102 on the physical and chemical characteristics of a single anticyclonic eddy observed ~900 km
103 offshore, off central Chile. We tracked the eddy back to its region of formation and
104 examined changes in concentration of oxygen and nitrogen species from the time it left the
105 coast to the time it was sampled in the oligotrophic ocean.

106 **METHODS**

107 **Hydrography and nitrogen data**

108 Hydrographic data and water samples for analyses of nutrients, N₂O and surface $\delta^{15}\text{N}$ -POM
109 were collected along a transect from Valparaíso, Chile (33°S, 71.6° W) to Easter Island (28.2°
110 S, 107.4° W) during the Tara Oceans Expedition (11 – 31 March 2011, Fig. 1; Karsenti et al.,
111 2011). Sampling consisted of 11 vertical profiles using a Sea-Bird 911 equipped with an
112 oxygen sensor (SBE43, sampling rate 24 Hz; Picheral et al., 2014). Due to logistical
113 constraints, the oxygen sensor could not be calibrated on board. It was calibrated at the
114 start of the expedition (July 2009) and a year later (August 2010 during a stopover in Cape
115 Town, South Africa). A third calibration was conducted in September 2011 (during a
116 stopover in Papeete). The sensor showed mean drifts of 0.101 (August 2010) and 0.405
117 $\mu\text{mol kg}^{-1}$ (September 2011), between successive calibrations. Because oxygen calibrations

118 could not be done routinely, post-cruise validation of oxygen data included comparison of
119 raw oxygen measurements with WOA13 climatology (Garcia et al., 2014) as described by
120 Roullier et al. (2014). For the ESP transect, absolute differences between measured
121 dissolved oxygen (SBE 43) and climatology for the upper 500 m of the water column
122 averaged $9.1 \mu\text{mol kg}^{-1}$ ($0.03 - 24.47 \mu\text{mol kg}^{-1}$) for oceanic stations and $16.7 \mu\text{mol kg}^{-1}$ (0.06
123 $- 36.24 \mu\text{mol kg}^{-1}$) for the coastal stations. Below 850m, absolute differences between in
124 situ measurements and climatology averaged $6.62 \mu\text{mol kg}^{-1}$ ($0.81 - 19.08 \mu\text{mol kg}^{-1}$).

125 Discrete water samples for N_2O (in triplicate) and nutrient (in duplicate) analyses were
126 obtained from a rosette equipped with 10 L Niskin bottles. Samples were collected at 0, 50,
127 100, 150, 200, 250, 300, 400, 500, and 900 m. N_2O samples (20 mL) were taken after the
128 inorganic carbon samples, using a tygon tubing to avoid bubble formation. Samples were
129 fixed with 50 μL of saturated mercuric chloride and stored in the dark. N_2O concentrations
130 were determined onshore using a gas chromatograph equipped with an electron capture
131 detector (ECD), following a headspace technique (McAullife, 1971). A four-point calibration
132 curve was determined with air (0.32 ppm) and N_2O standards of 0.1, 0.5 and 1 ppm (Scotty
133 gas mixture; Air Liquid Co.).

134 Nutrient samples (NO_3^- , NO_2^- and PO_4^{3-}) were collected by filtering seawater (GF/F 0.7 μm
135 filters); filtrates were stored at -20°C until analysis onshore. Concentrations of NO_3^- , NO_2^-
136 and PO_4^{3-} were measured using a Seal Analytical AA3 AutoAnalyzer (Grasshoff et al., 1983).

137 Eddy identification and tracking

138 Presence and position of mesoscale eddies in the region was determined by analyzing
139 weekly maps of anomalies in sea level and geostrophic velocities from the multi-satellite
140 AVISO product (Ssalto/Duacs, <http://www.aviso.oceanobs.com/duacs/>), from April 2010 to
141 September 2011. This gridded, multi-satellite altimeter product provides spatial resolution
142 of $1/3^\circ$ and allows resolution of eddies with an e-folding scale > 40 km (Chaigneau et al.,
143 2011; Chelton et al., 2011). For eddy tracking, we used the Okubo-Weiss parameter method
144 (W), which evaluates the relative dominance of strain and vorticity (Chelton et al., 2007;
145 Okubo, 1970; Sangrà et al., 2009; Weiss, 1991):

146
$$W = S_n^2 + S_s^2 - \omega^2 \quad (1)$$

147 With

148
$$S_n = \frac{\partial u}{\partial x} - \frac{\partial v}{\partial y}; \quad (2)$$

149
$$S_s = \frac{\partial v}{\partial x} + \frac{\partial u}{\partial y}; \quad (3)$$

150
$$\omega = \frac{\partial v}{\partial x} - \frac{\partial u}{\partial y}; \quad (4)$$

151 where, S_n and S_s are the normal and shear components of strain, respectively, and ω is the
152 relative vorticity.

153 This approach confirmed that the water mass sampled in station 094-A (30°S , 81°W ;
154 TARA_20110316T1152Z_999_EVENT_CAST;
155 <http://doi.pangaea.de/10.1594/PANGAEA.836473>; Fig. 1a) was associated with an eddy. The

156 path of this eddy was reconstructed from its time of origin (28 April 2010) to the time of its
157 decay (29 June 2011) by tracing the eddy center (i.e., the region with highest vorticity) in
158 successive geostrophic fields.

159 Vertical hydrographic profiles obtained from station 094-A (within the identified eddy) were
160 compared with vertical profiles of temperature, salinity and dissolved oxygen concentration
161 collected during other studies in the area and with nearby Argo buoy profiles and
162 climatological information from WOA13 data (Garcia et al., 2014). Data available for the
163 nearest grid ($1^\circ \times 1^\circ$) to station 094-A were used in this analysis.

164 **Glider information at the origin of the eddy**

165 To characterize the properties of water near the time and location of eddy formation we
166 used temperature, salinity and oxygen data from a cross-shore transect ($73.0 - 74.8^\circ$ W,
167 36.5° S) conducted with a Slocum glider (Teledyne Technologies) in June 2010 (Pizarro et
168 al., 2015). The data covered an area that extended to within 160 km from the presumed
169 starting point of the eddy based on satellite backtracking. The glider was equipped with an
170 optical oxygen sensor (Aanderaa Data Instrument oxygen Optode model 3830). Oxygen
171 sensor calibrations are routinely done at the Physical Oceanography Laboratory,
172 Universidad de Concepción, with a two-point calibration (0% and 100% of oxygen
173 saturation). Details of the sensor and the physical principles involved in the measurements
174 are described in Körtzinger et al. (2005) and Uchida et al. (2008).

175 RESULTS AND DISCUSSION

176 Hydrography

177 A vertical section of temperature, salinity and oxygen, measured along the transect from
178 Valparaíso (33.4° S, 71.6° W) to Easter Island (27.08° S, 109.3° W) in March 2011 provides
179 regional context (Fig. 1b, 1c, 1d, respectively). A subsurface oxygen minimum layer (with
180 dissolved oxygen concentration as low as $1.17 \mu\text{mol O}_2 \text{ kg}^{-1}$) was detected at station 094-A,
181 922 km offshore (30°S, 81°W, Fig. 1d). Dissolved oxygen concentrations observed at 094-A
182 are anomalous given that at this latitude the boundary of the OMZ (defined as $\text{O}_2 < 44.6$
183 $\mu\text{mol kg}^{-1}$) and its core (defined as $\text{O}_2 < 22.3 \mu\text{mol kg}^{-1}$) do not typically extend beyond ~ 600
184 km and ~ 500 km from the shoreline, respectively (Silva et al., 2009). Suboxic conditions ($\text{O}_2 <$
185 $10 \mu\text{mol kg}^{-1}$), are thought to be confined to the shelf region and were reported only in some
186 bottom waters over the continental shelf (Farías, 2003). Climatological data indicate that
187 subsurface water in the vicinity of station 094-A is typically oxygenated (Fig. 1e). According
188 to above classification of dissolved oxygen concentrations, the OMZ observed at station
189 094-A has its upper and lower boundaries at depths of 164 and 536 m, respectively, while
190 suboxic conditions were observed between 174 m and 421 m (66% of the OMZ).

191 The low-oxygen water mass was associated with higher salinities (34.60 – 34.66) compared
192 to surrounding water (Fig. 1c) and climatology for this region (34.15 – 34.36, for the years
193 1965 - 2012). Historical data from previous cruises conducted along the P06-WOCE transect
194 (32.5° S) or north of the study region (e.g., 28°S, Scorpio; Silva et al., 2009; 27°S, CIMAR 5
195 cruise Fuenzalida et al., 2006) do not show such anomalies in physical and chemical

196 conditions at this longitude (Fig. 2a and 2b). The presence of the anomalous salinity
197 signature observed in this study is supported by an independent Argo float that profiled in
198 the vicinity of 094-A (33.86° S, 79.84° W) during the Tara Oceans' sampling period (Fig. 2).

199 Vertical profiles of salinity and temperature anomalies at 094-A show a warm and salty core
200 centered between 230 and 270 m, accompanied by the dome and bowl shapes of the upper
201 and lower thermocline, respectively (Fig. 3). This feature is characteristic of an
202 intrathermocline, anticyclonic eddy (ITE, Xiu and Chai 2011; Chaigneau et al., 2011;
203 Hormazábal et al., 2013). Positive sea-level anomalies (SLA) and associated geostrophic
204 currents further indicate that station 094-A was located close to the center of a mesoscale
205 anticyclonic eddy (~ 150 km in diameter), centered at 33.45°S, 80.85°W (Fig. 4).

206 Reconstruction of this mesoscale eddy suggests that it was formed in the coastal transition
207 zone off Concepción (36.09° S, 74.21° W), approximately 315 d prior to our sampling at
208 station 094-A, and advected northwest at a mean velocity of 2.4 cm s^{-1} , approx. 2 Km d^{-1}
209 (Fig. 4). Reconstruction of the eddy's velocity and direction agrees well with previously
210 reported trajectories of eddies in the area (Chaigneau, 2005).

211 **OMZ evolution in the eddy**

212 In the ESP, eddies could frequently transport suboxic water from the coastal OMZ to oceanic
213 regions (Hormazábal et al., 2013). Low-oxygen water masses ($\text{O}_2 < 44.6 \text{ } \mu\text{M}$) have been
214 detected in the middle of the South Pacific Ocean (2000 km offshore at 28°S; Silva et al.,
215 2009), but at the time the authors did not associated these water masses with mesoscale
216 eddies. In the North Pacific Ocean, low concentrations of dissolved oxygen in the subsurface

217 open ocean have been previously described in association with anticyclonic mesoscale
218 eddies (Altabet et al., 2012; Chaigneau et al., 2011; Johnson and McTaggart, 2010; Lukas
219 and Santiago-Mandujano, 2001), and have been attributed to low-oxygen source waters
220 (Lukas and Santiago-Mandujano, 2001) or to local consumption during the transport of an
221 eddy (Karstensen et al., 2015).

222 To estimate temporal changes in concentrations of dissolved oxygen in the subsurface layer
223 of our sampled eddy, we used underwater glider measurements, collected in June 2010, at
224 36.5°S / 74° W (120 km from shore). This is the estimated location of the eddy one month
225 after its formation and oxygen concentrations of source water are in agreement with those
226 reported for other ITEs in the same region (Hormazábal et al. 2013). Glider measurements
227 of dissolved oxygen showed a well-developed OMZ ($O_2 < 44.6 \mu\text{M}$; Fig. 5) between 104 and
228 352 m, with a suboxic layer located between 135 and 226 m. We refer to these values as
229 the eddy's 'initial' subsurface oxygen concentrations. Dissolved oxygen concentrations
230 were then compared along isopycnals between the estimated location of the eddy's origin
231 and its offshore location at station 094-A (Fig. 6). By the time the eddy reached its offshore
232 location, the OMZ in the eddy was deeper and thicker (located between 164 and 537 m)
233 than the OMZ measured in the coastal transition zone, and the lowest dissolved oxygen
234 concentration decreased from $7.34 \mu\text{mol kg}^{-1}$ at 173 m to $1.17 \mu\text{mol kg}^{-1}$ at a depth of 338
235 m. The suboxic layer of the eddy in the open-ocean was located between 174 and 422 m,
236 almost three times thicker than the suboxic layer of the "source water" (Fig. 6). This
237 suggests that the observed OMZ offshore is a result of both advection of low-oxygen coastal
238 water by an eddy and continuing biological consumption during its transport. Estimated

239 oxygen consumption rate in the OMZ of the eddy ranged from 0.29 to 44 nmol O₂ L⁻¹ d⁻¹
240 (~0.1 - 15 μmol O₂ L⁻¹ yr⁻¹) in the core of the eddy (Fig. 6), which is quite high compared to
241 previously reported oxygen consumption rates in other OMZs in this depth range
242 (Karstensen et al., 2008). Considering the eddy's area (20 × 10³ km²; transport of ESSW of
243 ~1.38 Sv) and the thickness of the layer with dissolved oxygen concentrations < 44.6 μM
244 (373 m), an oxygen deficit of 12.2 Tg is expected in the subsurface eddy's layer. This
245 calculation is likely to underestimate the oxygen deficit since mixing with surrounding
246 oxygen-rich water has not been taken into account here. If the whole sub-saturated oxygen
247 layer of the eddy is considered (from ~80 to 1000m), the estimated oxygen deficit
248 transported to the oceanic region is even larger. While this crude, back-of-the-envelope
249 calculation of oxygen deficit should be taken with a grain of salt, it highlights the significant
250 influence of eddies on OMZs in the open ocean. When the eddy dissipates, the oxygen
251 deficit in the subsurface layer will be redistributed and will contribute to the overall oxygen
252 budget of the ESP OMZ region.

253 The area of the 'birth' of the studied eddy (~36°S) has been identified as a hotspot of eddy
254 generation (Hormazábal et al., 2013), with ~ 5-7 ITEs that can reach a diameter > 100 km
255 being formed every year. If the eddy studied here is representative of eddies generated in
256 the OMZ of the eastern boundary of the Pacific Ocean, between 31° and 36° S, advection of
257 and continued respiration within oxygen-deficient waters could produce a deficit as high as
258 60 – 85 Tg O₂ yr⁻¹ within the oceanic region.

259 Subsurface biogeochemical implications of the eddy

260 OMZ regions of eastern boundary current systems are considered important with respect
261 to the nitrogen cycle. These are areas where nitrogen is lost due to denitrification and
262 anammox, and are often associated with buildup of nitrite (NO_2^- ; Lam and Kuypers, 2011).
263 Water masses with these features can be advected and the processes enhanced offshore
264 as indicated by the observed accumulation of high subsurface NO_2^- in anticyclonic coastal
265 eddies (Stramma et al., 2013).

266 Off the Chilean coast, elevated NO_2^- concentrations are generally found within the core of
267 the OMZ (Cornejo and Farías, 2012a; Silva et al., 2009). Previous studies conducted in the
268 region of the eddy's formation show that nitrite concentrations in hypoxic waters ($< 7 \mu\text{mol}$
269 $\text{O}_2 \text{ kg}^{-1}$) are $< 0.1 \mu\text{M}$ (Cornejo and Farías, 2012b). In the present study, initial oxygen
270 concentrations in the OMZ of the eddy were low enough to support high denitrification and
271 anammox and, consequently, the accumulation of NO_2^- . The vertical distribution of NO_2^- in
272 station 094-A (oligotrophic ocean) shows a subsurface NO_2^- maximum (up to $0.56 \mu\text{M}$) at a
273 depth of 250 m (Fig. 1f). The apparent buildup of NO_2^- concentration within the eddy
274 corresponds to a NO_3^- deficit (N^*) of $-13.90 \mu\text{M}$ (Fig. 6) relative to surrounding water
275 (determined from the deviation of the $\text{NO}_3^-:\text{PO}_4^{3-}$ molar ratio from the Redfield ratio
276 according with Deutsch et al., 2001), suggesting that conditions in the eddy's anoxic zone
277 were favorable for denitrification. A subsurface water mass with low oxygen concentrations
278 and marked nitrate deficit has been previously observed in the oligotrophic, oceanic water
279 of the EPS, during the Scorpio cruise (Fig. 7, Silva et al., 2009), but other nitrogen species

280 indicative of denitrification were not measured, and tools to link this water mass to eddy
281 activity were not well developed at that time.

282 Another indication of the existence of anaerobic conditions within the OMZ of the eddy is
283 the presence of a N₂O consumption layer. This greenhouse gas is produced by nitrification
284 and denitrification under hypoxic conditions and consumed by denitrification under suboxic
285 conditions (< 8 μM of O₂; Bonin et al., 1989). The vertical distribution of N₂O in the eddy
286 (station 094-A) shows a double peak with a supersaturation at the upper and lower
287 boundaries of the subsurface OMZ (up to 224%) and subsaturation (44%) in the upper
288 region of the OMZ core (Fig. 1e), suggesting that both production and consumption of N₂O
289 occurred in the eddy. Layers depleted in N₂O have been previously observed in different
290 OMZs in coastal environments where denitrification takes place (Cornejo and Farías,
291 2012a). To the best of our knowledge, this is the first reported N₂O consumption layer in
292 oceanic subsurface waters of the South Pacific Ocean.

293 Oxygen concentrations in the area where the eddy was formed are often too high to support
294 significant N₂O consumption (Cornejo and Farías, 2012b; Cornejo et al., 2015). Thus N₂O is
295 being accumulated alongshore in the coastal OMZ (up to 25 nM) and consumed only in
296 bottom waters associated with suboxic conditions. In the absence of direct measurements
297 of N₂O concentrations at the time of eddy formation, we use the mean coastal N₂O
298 concentrations (22.68 ± 2.99 nM) from three previous cruises (FIP; Cornejo et al., 2015)
299 observed at the isopycnal $\sigma_t = 26.56 \text{ kg m}^{-3}$ (depth with N₂O undersaturation at station 094-
300 A) as the 'initial' concentration of N₂O in the eddy. We estimated a consumption rate of

301 3.92 nmol N₂O L⁻¹ d⁻¹ during the time the eddy was advected offshore. This N₂O
302 consumption rate is half of those reported from incubation experiments conducted at the
303 upper (shallower) boundary of the OMZ off Perú (8.16 nmol L⁻¹ d⁻¹; Dalsgaard et al., 2012).
304 Higher rates might have occurred in the center of the eddy, where more active
305 denitrification is expected. Furthermore, it is likely that we have underestimated N₂O
306 production since mixing with upper and lower layers that are supersaturated with respect
307 to N₂O, was not taken into account in our calculation.

308 Although N₂O was sampled from discrete depths, the thickness of the N₂O consumption
309 layer can be estimated considering that N₂O consumption does not occur at dissolved
310 oxygen concentrations > 8 µM (Bonin et al., 1989). Within the eddy, this layer was 60 m
311 thick (210 – 270 m) meaning that net consumption was at least ~ 0.15 Gg N₂O during the
312 offshore transfer. This N₂O consumption represents only 14% of the N₂O accumulation
313 estimated above and below the consumption layer, suggesting that the eddy provided a net
314 supply of ~0.85 Gg of N₂O to the oceanic region. Observing both production and
315 consumption of N₂O in the eddy signifies net nitrogen loss, with possible impacts on even
316 global nitrogen and N₂O balances.

317 This study provides new evidence that anticyclonic mesoscale eddies play important roles
318 in the biogeochemistry of the ESP (Altabet et al., 2012; Stramma et al., 2013). Previous
319 studies have shown that mesoscale eddies act as hotspots for microbially mediated nitrogen
320 loss via denitrification in coastal water; here we show that open-ocean anticyclonic eddies
321 can play a similar role in parts of the ocean that are far removed from productive coastal
322 waters and their associated OMZs.

323 **ACKNOWLEDGMENT**

324 This study is partly based on datasets gathered by the Tara Oceans Expeditions 2009-2012.
325 We are keen to thank the committed people and the following sponsors who made this
326 singular expedition possible: CNRS, EMBL, Genoscope/CEA, ANR, agnès b., the Veolia
327 Environment Foundation, Region Bretagne, World Courier, Cap l’Orient, the Foundation EDF
328 Diversiterre, FRB, the Prince Albert II de Monaco Foundation, Etienne Bourgois and the Tara
329 schooner, crew. Moreover, this integrated sampling strategy couldn’t have been done
330 without the involvement of École Normale Supérieure, Université Pierre et Marie Curie,
331 Stazione Zoologica, University College Dublin, University of Milan-Bicocca, Institute de
332 Ciencias del Mar, University of Bremen, Institute de Microbiologie de la Mediterranée,
333 MNHN, MIT, UofA, Bigelow Institute, Universite Libre de Bruxelles, University of Hawaii. We
334 thank Sarah Searson for providing technical support onboard, Marc Picheral for calibrations
335 of the oxygen sensor and Sabrina Speich for providing satellite images that helped guiding
336 sampling during the cruise. We thank Peter Jumars and John Dolan for his helpful comments
337 and edits. This work is part of the Millennium Scientific Initiative, grant IC 120019. M. Ramos
338 and L. Bravo are grateful for support from Chilean Millennium Initiative (NC120030) grant.
339 L. Bravo acknowledges support from Posdoctoral-FONDECYT/Chile-3130671. O. Pizarro
340 thanks support from FONDECYT 11021041, PFB 37/02 and MI-LOCO (Gordon and Betty
341 Moore Foundation). J. Karstensen was supported by the DFG project SFB 754
342 (<http://www.sfb754.de>). M. Correa-Ramirez was supported by FONDECYT N° 11130463. L.
343 Farias was supported by FONDAP program N° 15110009. The authors thank the Goddard
344 Space Flight Center, Greenbelt, MD 20771, USA, for the production and distribution of

345 MODIS data. SLA data were produced by Ssalto/Duacs and distributed by Aviso
346 <http://www.aviso.oceanobs.com/duacs/>. *This article is contribution number ZZZ of Tara*
347 *Oceans.*

348

REFERENCES

- Altabet, M. a., Ryabenko, E., Stramma, L., Wallace, D. W. R., Frank, M., Grasse, P. and Lavik, G.: An eddy-stimulated hotspot for fixed nitrogen-loss from the Peru oxygen minimum zone, *Biogeosciences*, 9(12), 4897–4908, doi:10.5194/bg-9-4897-2012, 2012.
- Bonin, P., Gilewicz, M. and Bertrand, J. C.: Effects of oxygen on each step of denitrification on *Pseudomonas nautica*., *Can. J. Microbiol.*, 35, 1061–1064, 1989.
- Chaigneau, A.: Eddy characteristics in the eastern South Pacific, *J. Geophys. Res.*, 110(C6), C06005, doi:10.1029/2004JC002815, 2005.
- Chaigneau, A., Le Texier, M., Eldin, G., Grados, C. and Pizarro, O.: Vertical structure of mesoscale eddies in the eastern South Pacific Ocean: A composite analysis from altimetry and Argo profiling floats, *J. Geophys. Res.*, 116(C11), C11025, doi:10.1029/2011JC007134, 2011.
- Chelton, D. B., Schlax, M. G., Samelson, R. M. and de Szoeke, R. a.: Global observations of large oceanic eddies, *Geophys. Res. Lett.*, 34(15), L15606, doi:10.1029/2007GL030812, 2007.
- Chelton, D. B., Schlax, M. G. and Samelson, R. M.: Global observations of nonlinear mesoscale eddies, *Prog. Oceanogr.*, 91(2), 167–216, doi:10.1016/j.pocean.2011.01.002, 2011.
- Cornejo, M. and Farías, L.: Following the N₂O consumption in the oxygen minimum zone of the eastern South Pacific, *Biogeosciences*, 9(8), 3205–3212, doi:10.5194/bg-9-3205-2012, 2012a.
- Cornejo, M. and Farías, L.: Meridional variability of the vertical structure and air–sea fluxes of N₂O off central Chile (30–40°S), *Prog. Oceanogr.*, 92-95, 33–42, doi:10.1016/j.pocean.2011.07.016, 2012b.
- Cornejo, M., Murillo, A. and Farias, L.: UNACCOUNTED N₂O SINK IN THE SURFACE WATER OF THE EASTERN SUBTROPICAL SOUTH PACIFIC, *Prog. Oceanogr.*, Aceptado, 2014.
- Dalsgaard, T., Thamdrup, B., Farías, L. and Peter Revsbech, N.: Anammox and denitrification in the oxygen minimum zone of the eastern South Pacific, *Limnol. Oceanogr.*, 57(5), 1331–1346, doi:10.4319/lo.2012.57.5.1331, 2012.
- Deutsch, C., Gruber, N., Key, R. M. and Sarmiento, J. L.: Denitrification and N₂ fixation in the Pacific Ocean, *Global Biogeochem. Cycles*, 15(2), 483–506, 2001.

Farías, L.: Remineralization and accumulation of organic carbon and nitrogen in marine sediments of eutrophic bays: the case of the Bay of Concepcion, Chile, *Estuar. Coast. Shelf Sci.*, 57(5-6), 829–841, doi:10.1016/S0272-7714(02)00414-6, 2003.

Fuenzalida, R., Schneider, W., Blanco, J. L., Garcés-Vargas, J. and Bravo, L.: Sistema de corrientes Chile-Perú y masas de agua entre Caldera e Isla de Pascua, *Com. Ocean. Nac.*, 2006.

Garcia, H. E., Locarnini, R. A., Boyer, T. P., Antonov, J. I., Baranova, O. K., Zweng, M. M., Reagan, J. R. and Johnson, D. R.: *WORLD OCEAN ATLAS 2013 Volume 3 : Dissolved Oxygen , Apparent Oxygen Utilization , and Oxygen Saturation.*, 2014.

Grasshoff, K., Ehrhardt, M. and Kremling, K.: *Methods of seawater analysis*, edited by K. Grasshoff, K. Kremling, and M. Ehrhardt, Verlag Chemie., 1983.

Gruber, N.: Warming up, turning sour, losing breath: ocean biogeochemistry under global change., *Philos. Trans. A. Math. Phys. Eng. Sci.*, 369(1943), 1980–96, doi:10.1098/rsta.2011.0003, 2011.

Hormazábal, S., Combes, V., Morales, C., Correa-Ramirez, M. a., Di Lorenzo, E. and Nuñez, S.: Intrathermocline eddies in the coastal transition zone off central Chile, 2013.

Johnson, G. C. and McTaggart, K. E.: Equatorial Pacific 13°C Water Eddies in the Eastern Subtropical South Pacific Ocean*, *J. Phys. Oceanogr.*, 40(1), 226–236, doi:10.1175/2009JPO4287.1, 2010.

Karsenti, E., Acinas, S. G., Bork, P., Bowler, C., De Vargas, C., Raes, J., Sullivan, M., Arendt, D., Benzoni, F., Claverie, J.-M., Follows, M., Gorsky, G., Hingamp, P., Iudicone, D., Jaillon, O., Kandels-Lewis, S., Krzic, U., Not, F., Ogata, H., Pesant, S., Reynaud, E. G., Sardet, C., Sieracki, M. E., Speich, S., Velayoudon, D., Weissenbach, J. and Wincker, P.: A holistic approach to marine eco-systems biology., *PLoS Biol.*, 9(10), e1001177, doi:10.1371/journal.pbio.1001177, 2011.

Karstensen, J., Stramma, L. and Visbeck, M.: Oxygen minimum zones in the eastern tropical Atlantic and Pacific oceans, *Prog. Oceanogr.*, 77(4), 331–350, 2008.

Karstensen, J., Fiedler, B., Schütte, F., Brandt, P., Körtzinger, A., Fischer, G., Zantopp, R., Hahn, J., Visbeck, M. and Wallace, W.: Open Ocean dead zone in the tropical North Atlantic Ocean, *Biogeosciences*, 12, 1–9, doi:10.5194/bg-12-1-2015, 2015.

Körtzinger, A., Schimanski, J. and Send, U.: High quality oxygen measurements from profiling floats: A promising new technique, *J. Atmos. Ocean. Technol.*, 22(3), 302–308, 2005.

Lam, P. and Kuypers, M. M. M.: Microbial Nitrogen Cycling Processes in Oxygen Minimum Zones, *Ann. Rev. Mar. Sci.*, 3(1), 317–345, doi:10.1146/annurev-marine-120709-142814, 2011.

Lukas, R. and Santiago-Mandujano, F.: Extreme water mass anomaly observed in the Hawaii Ocean Time-series, *Geophys. Res. Lett.*, 28(15), 2931–2934, 2001.

McAullife, C.: GC determination of solutes by multiple phase equilibration, *Chem. Technol.*, 1(1), 46–51 [online] Available from: <http://www.csa.com/partners/viewrecord.php?requester=gs&collection=ENV&recid=7105344>, 1971.

McGillicuddy, D., Robinson, A., Siegel, D., Jannasch, H., Johnson, R., Dickey, T., McNeil, J., Michaels, A. and Knap, A.: Influence of mesoscale eddies on new production in the Sargasso Sea, *Nature*, 395, 263–266, 1998.

Morales, C. E., Loreto Torreblanca, M., Hormazabal, S., Correa-Ramírez, M., Nuñez, S. and Hidalgo, P.: Mesoscale structure of copepod assemblages in the coastal transition zone and oceanic waters off central-southern Chile, *Prog. Oceanogr.*, 84(3-4), 158–173, doi:10.1016/j.pocean.2009.12.001, 2010.

Morales, C. E., Hormazabal, S., Correa-Ramírez, M., Pizarro, O., Silva, N., Fernandez, C., Anabalón, V. and Torreblanca, M. L.: Mesoscale variability and nutrient–phytoplankton distributions off central-southern Chile during the upwelling season: The influence of mesoscale eddies, *Prog. Oceanogr.*, 104, 17–29, doi:10.1016/j.pocean.2012.04.015, 2012.

Okubo, A.: Horizontal dispersion of floatable particles in the vicinity of velocity singularities such as convergences*, *Deep Sea Res.*, 17, 445–454, 1970.

Picheral, M., Searson, S., Taillandier, V., Bricaud, A., Boss, E., Stemmann, L., Gorsky, G. and Consortium, Tara Oceans Coordinators Tara Oceans Expedition, P.: Vertical profiles of environmental parameters measured from physical, optical and imaging sensors during Tara Oceans expedition 2009-2013, *pangaea*, doi:10.1594/PANGAEA.836321, 2014.

Pizarro, G., Montecino, V., Astoreca, R., Alarcón, G., Yuras, G. and Guzmán, L.: Variabilidad espacial de condiciones bio-òpticas de la columna de agua entre las costas de Chile insular y continental. Primavera 1999 y 2000, *Cienc. y Tecnol. Mar.*, 29(1), 45–58, 2006.

Roullier, F., Berline, L., Guidi, L., Sciandra, A., Durrieu De Madron, X., Picheral, M., Pesant, S. and Stemmann, L.: Particles size distribution and carbon flux across the Arabian Sea Oxygen Minimum Zone, *Biogeosciences Discuss.*, 10(12), 19271–19309, doi:10.5194/bgd-10-19271-2013, 2014.

Sangrà, P., Pascual, A., Rodríguez-Santana, Á., Machín, F., Mason, E., McWilliams, J. C., Pelegrí, J. L., Dong, C., Rubio, A., Arístegui, J., Marrero-Díaz, Á., Hernández-Guerra, A., Martínez-Marrero, A. and Auladell, M.: The Canary Eddy Corridor: A major pathway for long-lived eddies in the subtropical North Atlantic, *Deep Sea Res. Part I Oceanogr. Res. Pap.*, 56(12), 2100–2114, doi:10.1016/j.dsr.2009.08.008, 2009.

Silva, N., Rojas, N. and Fedele, A.: Water masses in the Humboldt Current System: Properties, distribution, and the nitrate deficit as a chemical water mass tracer for Equatorial Subsurface Water off Chile, *Deep Sea Res. Part II Top. Stud. Oceanogr.*, 56(16), 1004–1020, doi:10.1016/j.dsr2.2008.12.013, 2009.

Stramma, L., Bange, H. W., Czeschel, R., Lorenzo, a. and Frank, M.: On the role of mesoscale eddies for the biological productivity and biogeochemistry in the eastern tropical Pacific Ocean off Peru, *Biogeosciences*, 10(11), 7293–7306, doi:10.5194/bg-10-7293-2013, 2013.

Stramma, L., Weller, R. A., Czeschel, R. and Bigorre, S.: Eddies and an extreme water mass anomaly observed in the eastern south Pacific at the Stratus mooring, *J. Geophys. Res. Ocean.*, 119(2), 1068–1083, 2014.

Sweeney, E. N., McGillicuddy, D. J. and Buesseler, K. O.: Biogeochemical impacts due to mesoscale eddy activity in the Sargasso Sea as measured at the Bermuda Atlantic Time-series Study (BATS), *Deep Sea Res. Part II Top. Stud. Oceanogr.*, 50(22-26), 3017–3039, doi:10.1016/j.dsr2.2003.07.008, 2003.

Uchida, H., Kawano, T., Kaneko, I. and Fukasawa, M.: In situ calibration of optode-based oxygen sensors, *J. Atmos. Ocean. Technol.*, 25(12), 2271–2281, 2008.

Weiss, J.: The dynamics of enstrophy transfer in two-dimensional hydrodynamics, *Phys. D Nonlinear Phenom.*, 48(2-3), 273–294, 1991.

Xiu, P. and Chai, F.: Modeled biogeochemical responses to mesoscale eddies in the South China Sea, *J. Geophys. Res.*, 116(C10), C10006, doi:10.1029/2010JC006800, 2011.

Table 1. Sources of hydrographic data used in this study. The name, location, and distance between the nearest location of the measurements and station 094-A are reported.

Name of the program	Year	Station	Location	Distance to 094-A [km]	Kind of data
P06E (WOCE) ¹	1992, 2003 2010	24	32.52° S/80.64°W	93.1	Profile
Biosope ²	2004	STB19	33.04° S/81.18°W	23.8	Profile
Float ARGO ³	2011	---	33.86° S/79.84°W	137.3	Float
WOA13 ²	Climatology	13237	33.50° S/81.50°W	41.7	

¹ <http://www.nodc.noaa.gov/woce>

² source: <http://www.nodc.noaa.gov/OC5/indprod.html>

³source: <http://www.coriolis.eu.org>

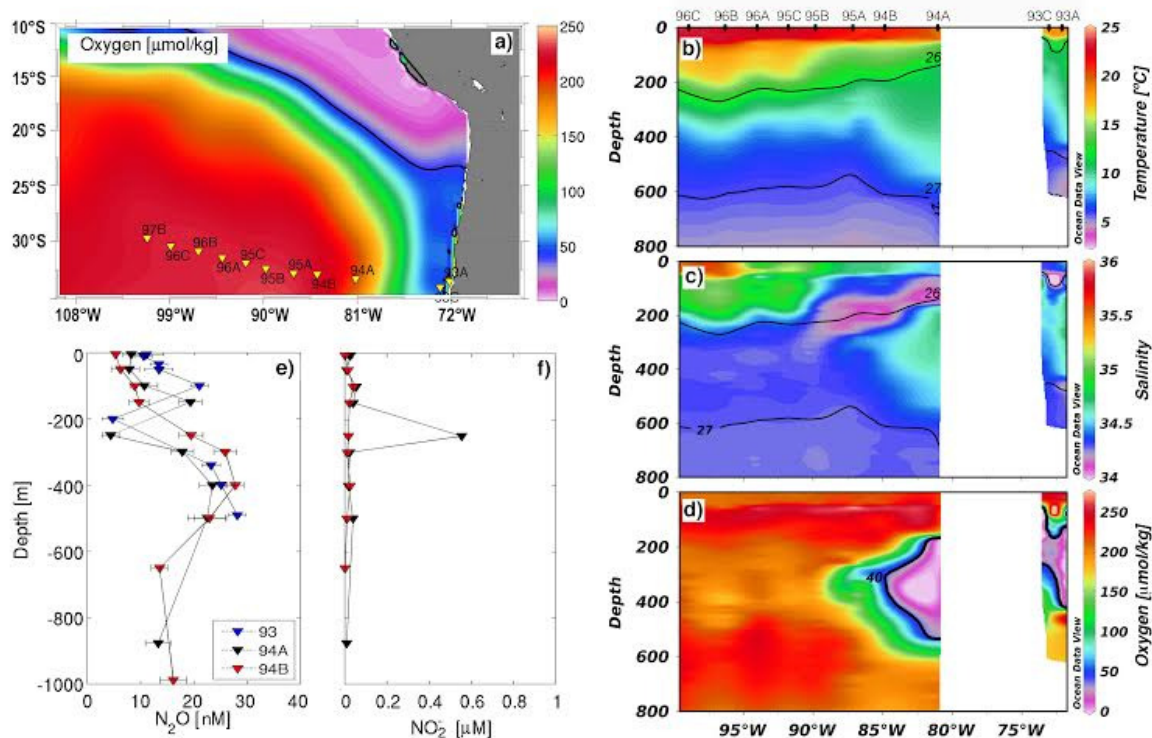


Figure 1. a) Climatology of dissolved oxygen distributions ($\mu\text{mol kg}^{-1}$) at a depth of 200 m in the eastern South Pacific Ocean. Yellow triangles indicate locations of stations during the Tara Oceans cruise. Vertical distributions of b) temperature ($^{\circ}\text{C}$) c) salinity and d) dissolved oxygen along the transect of the Tara Ocean cruise, from coastal water off Chile to the open ocean. Black lines in b) and c) indicate the 26.0 and 27.0 $\text{kg m}^{-3}\sigma_t$ isopycnals. Black line in d) indicates the isoclines of 40 $\mu\text{mol kg}^{-1}$ of dissolved oxygen. e) Vertical distribution of N_2O at Tara stations 093 ($34.0^{\circ}\text{S} / 73.0^{\circ}\text{W}$, blue triangles; TARA_20110312T1637Z_093_EVENT_CAST), 094-A ($33.2^{\circ}\text{S} / 81.1^{\circ}\text{W}$, black triangles; TARA_20110316T1152Z_999_EVENT_CAST) and 094-B ($32.8^{\circ}\text{S} / 84.8^{\circ}\text{W}$, red triangles; TARA_20110317T1815Z_999_EVENT_CAST). f) Vertical distribution of NO_2^- at Tara stations, 094-A (black triangles) and 094-B (red triangles). For a complete detail of the Tara CTD cast please refer to (Picheral et al., 2014).

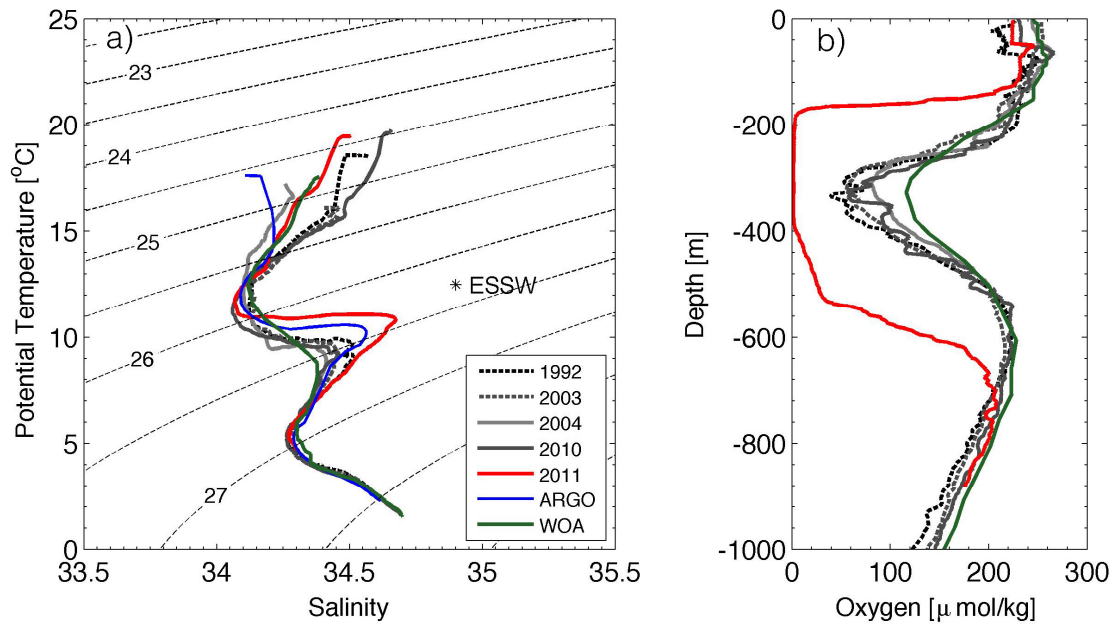


Figure 2.a) T-S diagram from various sampling programs in the study area; b) Dissolved oxygen profiles at Tara station 094-A (red line) and stations in its vicinity from cruises conducted on 1992 (black dashed line), 2003 (gray dashed line), 2010 (thick gray line) and 2004 (thin gray line); from Argo buoys (blue line, without oxygen), and the WOA 2013 climatology (green line). More detail on data sources are provided in Table 1.

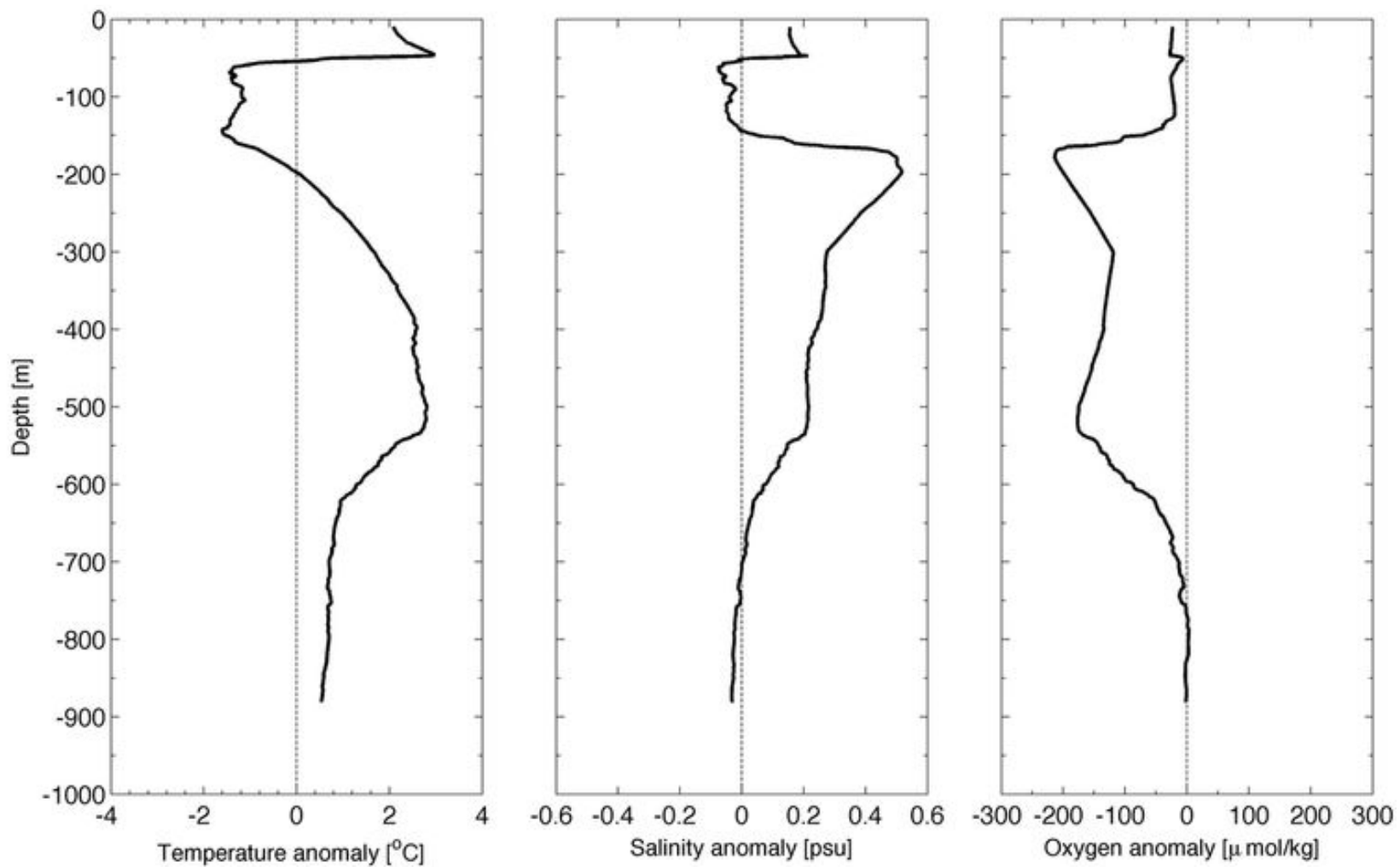


Figure 3. Vertical anomalies of: a) temperature (°C), b) Salinity, c) dissolved oxygen ($\mu\text{mol kg}^{-1}$) in station 094-A compared with WOA 2013 climatology (range of years for climatology).

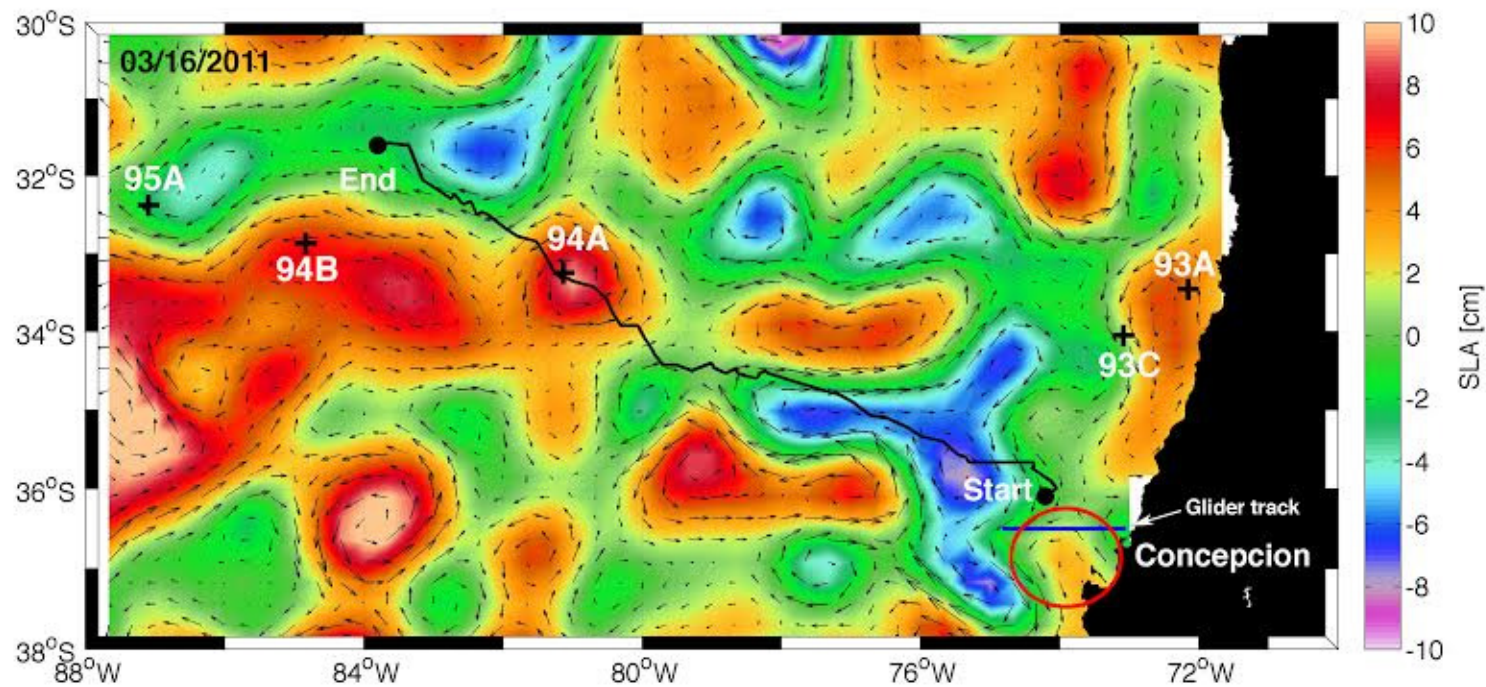


Figure 4. Sea surface height from satellite data at the time of sampling in Tara station 094-A (March 2011). The position of the sampling stations (black crosses) and estimated eddy trajectory (black line) with start and end locations (black circles) of the trajectory are also indicated. The red circle off Concepción (36°S) shows the probable eddy generation zone

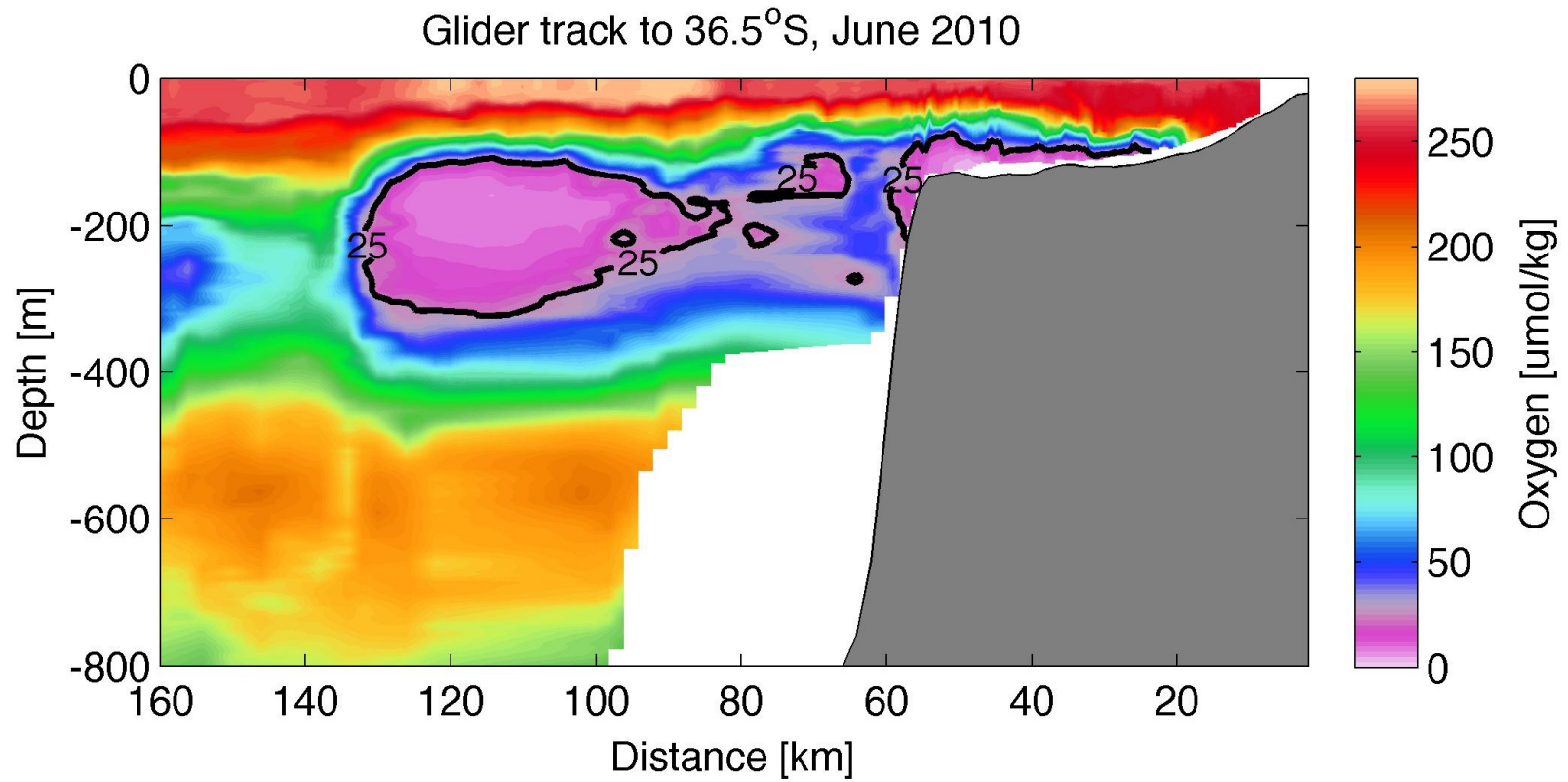


Figure 5. Vertical distributions of dissolved oxygen ($\mu\text{mol kg}^{-1}$) in a cross-shore section at 36.5°S near the time of eddy formation (June 2010). Black line indicates the isoline of 25 $\mu\text{mol kg}^{-1}$.

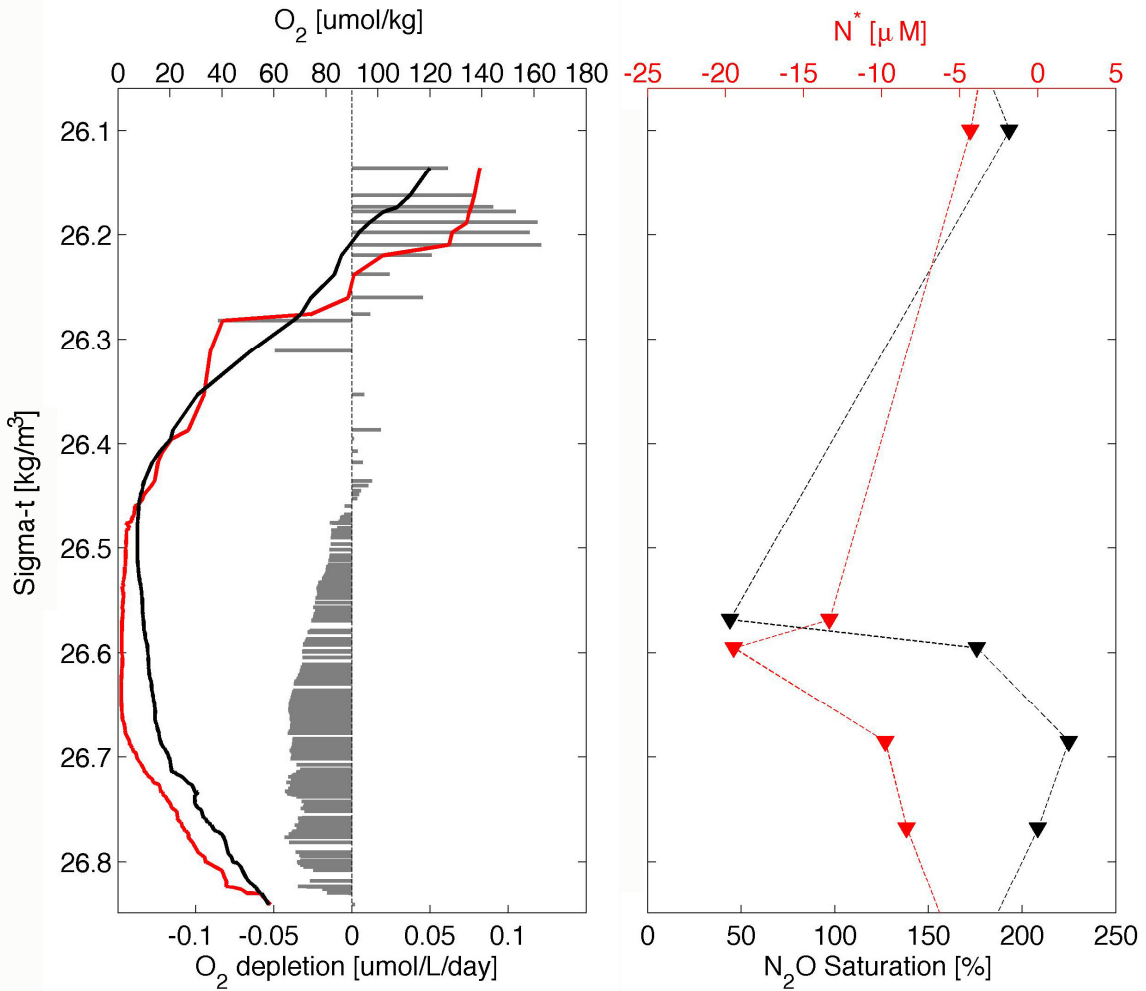


Figure 6. a) Vertical distribution of Oxygen as a function of sigma-t at Tara station 094-A (within the eddy) in March 2011 (red line) and at the coast in June 2010 (black line). Estimated O_2 depletion rates are shown as gray bars, where the vertical dotted line marks zero O_2 consumption rate. b) Vertical distributions of Nitrate deficit (N^*) and Nitrous oxide saturation (black triangles and line) as a function of sigma-t within the eddy at station 094-A.

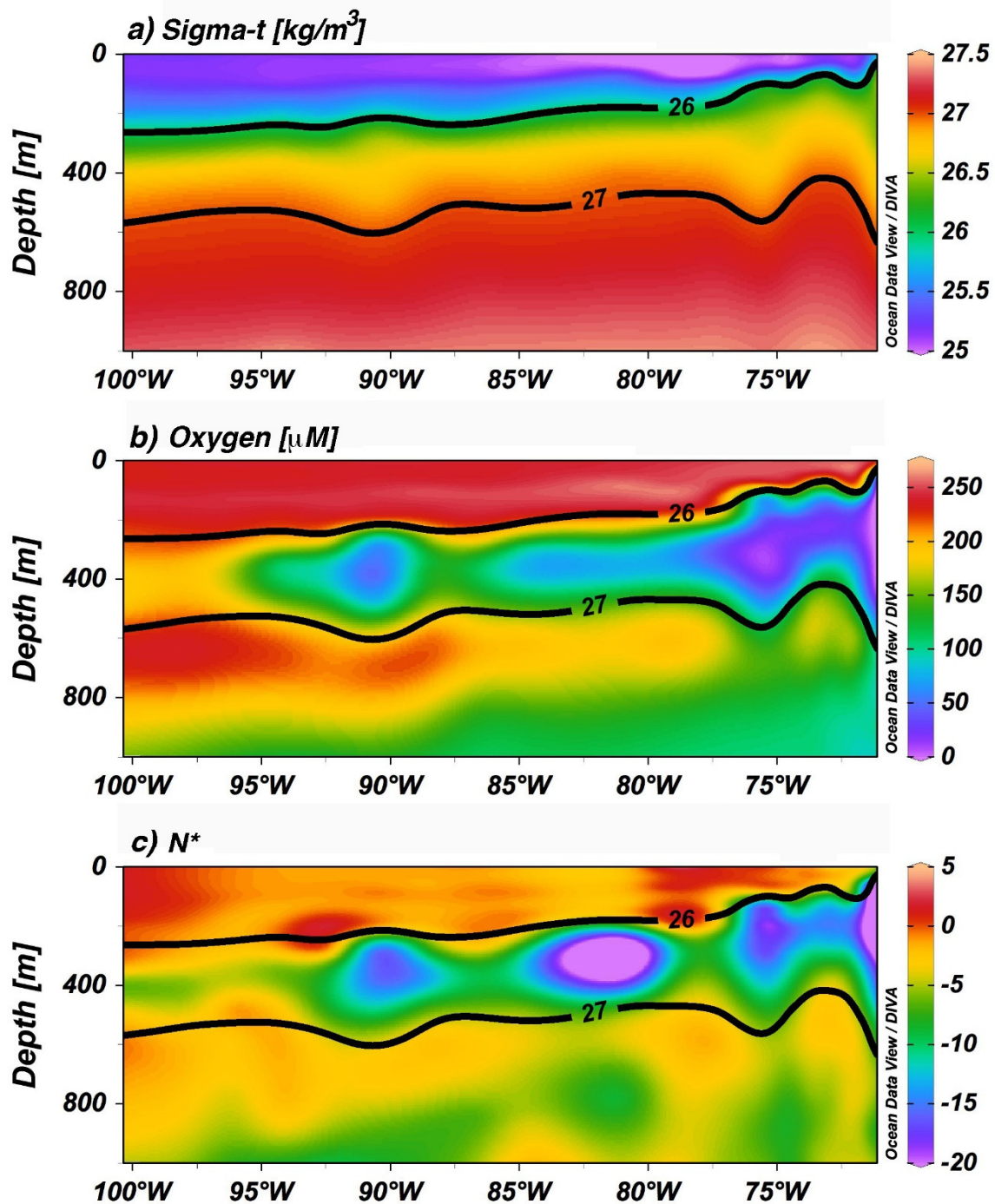


Figure 7. Vertical distributions of sigma-t, dissolved oxygen and nitrate deficit (N^* ; according to Deutsch et al., 2001) in a cross-shore transect along 28°S in the Eastern Southern Pacific Ocean (72° to 100° S) during Scorpio cruise (June 1967). Black lines refer to sigma-t of 26 and 27 kg m⁻³.